Prediction of the Effect of Ti on the (111) and (100) Antiphase Boundary Energy in Ni3Al

Materials Transactions, JIM, Vol. 40, No. 11 (1999), pp. 1301 to 1305
Special Issue on Advances in Computational Materials Science and Engineering

Prediction of the Effect of Ti on the (111) and (100) Antiphase Boundary Energy in Ni_3Al

Hai-Ping Wang, Marcel Sluiter and Yoshiyuki Kawazoe

Institute for Materials Research, Tohoku University, 980-8577 Sendai, Japan.

Segregation behavior of Ti impurities at (111) and (100) antiphase boundaries in Ni_3Al is computed and related to other phenomena associated with substitutional impurities in ordered intermetallic compounds. A relationship concerning site preference and segregation behavior is described.

(Received May 27, 1999; In final Form August 5, 1999)

Keywords: *antiphase boundary, impurity, segregation, antiphase boundary energy, Ni_3Al, cluster variation method*

I. Introduction

The most common post-1950 superalloys are nickel based with approximately 30 to 40 vol% Ni_3Al[1]. Ni_3Al has the $L1_2$ structure[2] that is derived from the fcc structure by ordering. In the $L1_2$ structure the cube corners are occupied by the Al species, and the face centers are occupied by the Ni species. The Ni_3Al phase forms precipitates whose size and morphology directly affect strength. Therefore, the study of the Ni_3Al phase is of considerable interest. The effect of Ti is of particular importance because Ni_3Al has a large solubility for Ti and the addition of Ti has been shown to increase oxidation resistance, high-temperature strength, and high-temperature creep resistance[1].

Antiphase boundaries (APBs) play an important role in the resistance to plastic deformation of intermetallic compounds such as Ni_3Al. The most important parameter which characterizes APBs is the APB energy (APBE). This property has been measured extensively, but the effect of composition and of impurities remains controversial[3][4]. Recent simulations of segregation of off-stoichiometric defects towards anti-phase boundaries (APB) in Ni_3Al have shown that the concentrations of Ni and Al in the immediate vicinity of the boundary can be 5 or more times farther from stoichiometry than in the surrounding bulk[4]. Therefore, a detailed study of the behavior of a substitutional impurity at APBs is in order. Here, the particular cases of Ti at (111) and (100) APBs in Ni_3Al are examined using the Cluster Variation Method (CVM) in the tetrahedron-octahedron (TO) approximation with *ab initio* effective interatomic interactions. This analysis should shed light also on the behavior of other early transition metal impurities, because these appear to behave in a rather similar manner[5][6].

II. Theory

In this study the cluster variation method (CVM) has been used to calculate configurational thermodynamic properties. The Helmholtz free energy F, expressed in term of internal energy U, temperature T, and entropy S,

$$F=U-TS, \tag{1}$$

is minimized with respect to the configurational degrees of freedom, such as site occupancies and correlation functions. In the CVM the internal energy and the entropy are given by a cluster expansion,

$$U^{CVM}=\sum_{\alpha}^{\alpha_{\max}} J_\alpha \xi_\alpha, \tag{2}$$

$$S^{CVM}=\sum_{\alpha}^{\alpha_{\max}} \gamma_\alpha S_\alpha, \tag{3}$$

where α represents a cluster, J an effective cluster interaction (ECI), ξ a correlation function, γ a Kikuchi-Barker coefficient[7], and S_α the entropy contribution from the cluster α. $\alpha_{\max}$ represents the maximal cluster that is considered in the expansion. The entropy contributions S_α are computed from a sum over all decorations σ of cluster α,

$$S_\alpha=-\sum_{\sigma_\alpha} p_{\sigma_\alpha} \log\,(p_{\sigma_\alpha}), \tag{4}$$

where p_σ is the probability for the occurrence of decoration σ. The probabilities take values between 0 and 1 and satisfy a normalization condition: $\Sigma_{\sigma_\alpha} p_{\sigma_\alpha}=1$. The probabilities are computed from the correlations functions[7],

$$p=C\xi, \tag{5}$$

using the configuration matrix C. As the correlation functions form a complete orthonormal basis, the free energy can be minimized with respect to ξ.

For perfectly ordered configurations the correlation functions can be determined simply by inspection. Therefore, when the energies $U^{(s)}$ of a set of structures (s) are known, eq. 2 can be inverted to obtain the ECI. This is the essence of the so-called Connolly-Williams method

(CWM)[7]. Here, a modified version of the CWM is used[8], in which J_α is calculated with

$$\sum_s w^s [U^s - \sum_{\alpha=1}^{\alpha_{max}} J_\alpha \xi_\alpha^\sigma]^2 = minimal, \quad (6)$$

where the weight w^s for each structure is set according to eq. (5) in Ref. (8). The factor w in that equation was set to 0.5.

The energies of a set of 58 fcc-based structures in the Ni–Al–Ti system were used to extract the ECI. For each of the three binary systems 17 structures as listed in Ref. (8) are selected as well as the following ternary structures: three $L1_p$ structures with compositions Ni_2AlTi, $NiAl_2Ti$, and $NiAlTi_2$, and the four structures shown in **Fig. 1** of Ref. (6). The last four structures are near the composition of interest, and provide insight in the site substitution behavior of Ti in Ni_3Al. The total energies were computed with the Linear Muffin-Tin Orbital method in the atomic sphere approximation (LMTO-ASA)[9]. Integrations in reciprocal space were carried out with the tetrahedron method using typically 1000 points as generated with the Monkhorst-Pack method[10] in the first Brillouin zone. The von Barth-Hedin exchange correlation parametrization was used. As maximal clusters for the cluster expansion and for the CVM calculations the TO approximation has been selected. It should be mentioned that only effects pertaining to the configurational Hamiltonian are considered here. The effects of atomic relaxation and vibrational excitations are not included in the calculations.

The thermodynamic properties of the APBs were modeled by a periodic replication of supercells. In the case of the (111) APB a supercell with translation vectors $\langle 1\bar{1}0\rangle$, $\langle 10\bar{1}\rangle$, $\langle 20\frac{1}{2}\ 19\frac{1}{2}\ 20\rangle$ in units of the $L1_2$ lattice parameter is employed. The (111) APBs in this cell are separated by 60 (111) planes from each other, so that effects up to 30 planes away from the center of an APB could be considered. The (100) APB was modeled in a supercell with translation vectors $\langle 100\rangle$, $\langle 010\rangle$, $\langle \frac{1}{2}\ \frac{1}{2}\ 20\rangle$ in units of the $L1_2$ lattice parameter. In this supercell the (100) APBs are separated by 40 (100) planes, which allows effects of up to 20 planes away from the APB to be evaluated. These cells were found to be adequately large for all cases. There were 10032 and 22686 independent correlation functions in the supercells pertaining to the (100) and (111) APBs, respectively. These correlation functions were optimized under the constraint of a fixed chemical potential. Thermodynamic properties of the APB were computed both with the difference method, and with the projector method[4], and in both cases identical results were found.

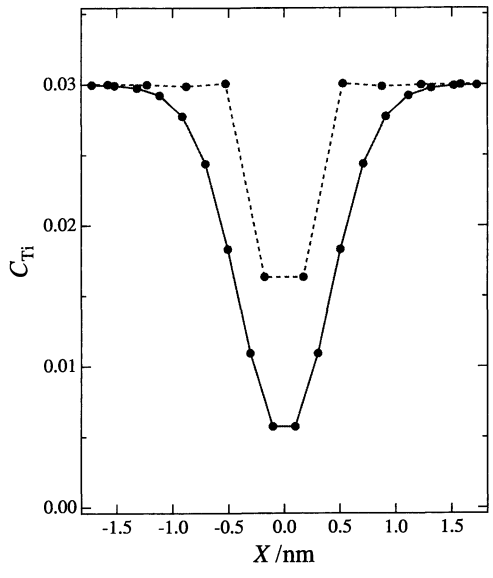

Fig. 1 Ti concentration C_{Ti} as a function of the distance X to the center of the APB in $Ni_{0.725}Al_{0.245}Ti_{0.030}$ at a temperature of 2000 K. (111) APB: solid line, and (100) APB: dashed line.

III. Results

For a ternary fcc alloy in the TO approximation there are 60 correlation functions, and hence, including the empty cluster, 61 effective cluster interactions are defined within this approximation. However, due to linear dependencies in the correlation functions of the crystal structures that were selected for the CWM, in fact, a singular value decomposition of eq. (6) yielded only 30 effective cluster interactions. All configurations were considered at one underlying fcc lattice parameter, namely that of the Ni_3Al $L1_2$ as computed with the LMTO-ASA (0.362 nm)[5]. This set of effective cluster interactions can reproduce the LMTO-ASA total energies with an error less than 50 meV/atom, and has a predictive error[8] of 100 meV/atom which is about 10% of the maximal formation energy in the system. Experience has shown that a predictive error of about 10% is sufficient to compute a phase diagram that strongly resembles the experimental diagram[8][11]–[13]. Here, the phase diagram was not calculated but it was verified that the cluster expansion produced the same ground states as had been found by the LMTO-ASA calculations. The computed Ni_3Al order-disorder temperature (T_c) is 2500 K, which is almost 1.5 times higher than the 1750 K estimated from extrapolation of ternary phase diagrams[14]. Fixing the lattice parameter at the equilibrium value of the ordered phase favors that phase over the disordered phase and this effect is in part responsible for the overestimated order-disorder temperature. The overestimation indicates that the ECIs may be somewhat too large. As there is a rough proportionality between T_c and the APBEs, this suggests that our APBEs too, may be overestimated. This appears indeed to be the case. As stated above, the ECIs allow the energy of any ordered configuration to be calculated. Thus, the APBE in stoichiometric Ni_3Al at 0 K on the (100) and (111) planes could be computed from only a knowledge of the atomic site occupancies. This gave APBEs of 318 mJ/m^2 for the (111) plane and 51 mJ/m^2 for the (100) plane. The (111) APBE is indeed larger than what other methods have given: Embedded atom method (EAM) calculations for positionally relaxed (111) APBs give an APBE only

half as large[15]-[17], while other LDA calculations, too, report lower values that are about 2/3 of the value calculated here[18]-[20]. The neglect of positional relaxations is partly responsible for the overestimation[21][4], and fixing the lattice parameter is a contributing factor.

The (100) APBE calculated here is between two EAM results, 83 mJ/m^2[16] and 28 mJ/m^2[17], but much lower than various LDA calculations, 140 mJ/m^2[18]. Experimental evidence too, suggests much larger values for the (100) APBE than was computed here[22]. Our low value for the (100) APBE can be directly related to the small energy difference between the Ni_3Al $L1_2$ and DO_{22} structures, because these two structures differ with each other in terms of closely spaced (100) APBs. The cluster expansion makes errors in the formation energies of the Ni_3Al $L1_2$ and DO_{22} structures such that the energy difference is only about a quarter of that in the LMTO-ASA. A better cluster expansion then would probably give much more reasonable values for the (100) APBE. Therefore, the small (100) APBE can be attributed to a shortcoming of the present cluster expansion. A possible method to improve the cluster expansion is to give large weights (see eq. (6)) to the $L1_2$ and DO_{22} structures. This will be explored in a future work. On purely geometric grounds it can be argued that generally the (111) APBE should be greater than the (100) APBE. Across a (111) APB, the nearest neighbor shell is disturbed. Therefore, the (111) APBE is proportional to the nearest neighbor ECI. At the (100) APB, however, the nearest neighbor shell is completely intact, and only in more distant shells is the coordination disturbed. As the nearest neighbor ECI generally is bigger than all other ECIs, and this is also the case in Ni_3Al, it follows that the (111) APBE is larger than the (100) APBE.

The finite temperature results obtained with the CVM give insight in the behavior of Ti in Ni_3Al. In agreement with previous work[5][6], Ti was found to have a strong site preference for the Al-type site. A previous calculation of the effective interatomic interactions[5] between Ni, Al and Ti revealed that Ti is strongly attracted to Ni and strongly repelled by Al. Although, the current cluster expansion with 30 ECI cannot easily yield such a simple description, the formation energies listed in **Table 1** indicate that the Ni–Ti bond is stronger than the Ni–Al bond in Ni_3Al based fcc alloys.

The nature of the interactions explains the strong site preference for the Al-site, because the Al site is surrounded by 12 Ni nearest neighbors, while the Ni site has 4 Al nearest neighbors and 8 Ni nearest neighbors. Clearly, when a Ti atom occupies an Al-type site, the number of attractive Ti–Ni bonds is greater, and the number of repulsive Ti–Al bonds is smaller, than the case is for a Ti located on a Ni-type site. As Al and Ti occupy the same sites, one can think of ternary $Ni_{3-x}Al_{1-y}Ti_{x+y}$ alloys as quasi-binaries, where the Al and Ti species occupy the Al-type sites, and Ni atoms occupy the Ni-type sites. An alloy can be called Ni-rich when the Ni concentration exceeds 75 a/o, and Ni-poor when the Ni concentration is less than 75 a/o.

Table 1 Formation energies of compounds based on the $L1_2$ structure, computed at the lattice parameter of the Ni_3Al phase (0.362 nm).

Composition	Structure	Formation energy (meV/atom)
Ni_3Al	$L1_2$	−745
Ni_6AlTi	*	−816
Ni_3Ti	$L1_2$	−838

*refers to the crystal structure shown in figure 1a of[6]

The same explanation also describes the behavior of Ti in the vicinity of an APB. In Fig. 1 the Ti concentration is shown as a function of the distance to the center of an APB in a material with a bulk composition $Ni_{0.725}Al_{0.245}Ti_{0.03}$. At other compositions and temperatures too, Ti is always found to strongly segregate away from the APB. Although the alloy in Fig. 1 is Ni-poor, which in a binary Ni-Al alloy would lead to a segregation of Ni away from the APB as a previous work[4] has shown, Ti does not segregate towards the APBs. Both Ni and Ti segregate away from the (100) and (111) APBs. The reason that Ni segregates away from the APBs in a binary alloy is basically that the other species, Al, is in excess. The excess Al forms antisite defects, and defects generally segregate towards areas where the order is disturbed such as at an APBs. Since Ti occupies the same site as Al, one might expect it to behave as Al, but that is not the case. Ti segregates away from the APB because the Al-type sites with perfect Ni coordination such as exist at some distance from the APB are energetically favorable over the Al-type sites near the APB, which do not have such perfect Ni coordination due to the disturbance of the local order. As both Ni and Ti segregate away from the APB, Al strongly segregates towards the APB. In fact, in a Ni-poor alloy the segregation of Al towards the APB is proportional to the Ti concentration, see **Fig. 2**. This occurs even when the alloy has an Al concentration below 25 a/o.

Generally, the segregation of all atomic species is stronger at the (111) APB than at the (100) APB. An explanation for this is the greater energies associated with (111) APBs than with (100) APBs. Another factor is again geometrical. In the case of a (100) APB there is an inert pure Ni layer that separates the two (100) planes which are shifted with respect to each other. Therefore, the (100) planes interact only through second neighbor interactions. These interactions are much weaker than the nearest neighbor interactions, so that the effect of the perturbation in the atomic order is not carried over as long a distance as is the case at (111) APBs. The width of the segregation profile is therefore much narrower for (100) APBs than for (111) APBs.

The APBE is shown as a function of composition and temperature in **Fig. 3**. Just as in the case of binary Ni-Al alloys, the APBE is maximal when the quasi-binary is stoichiometric, that is when the sum of the Al and Ti concentrations approaches 1/4. In agreement with the Gibbs absorption equation, Ti segregates away from the

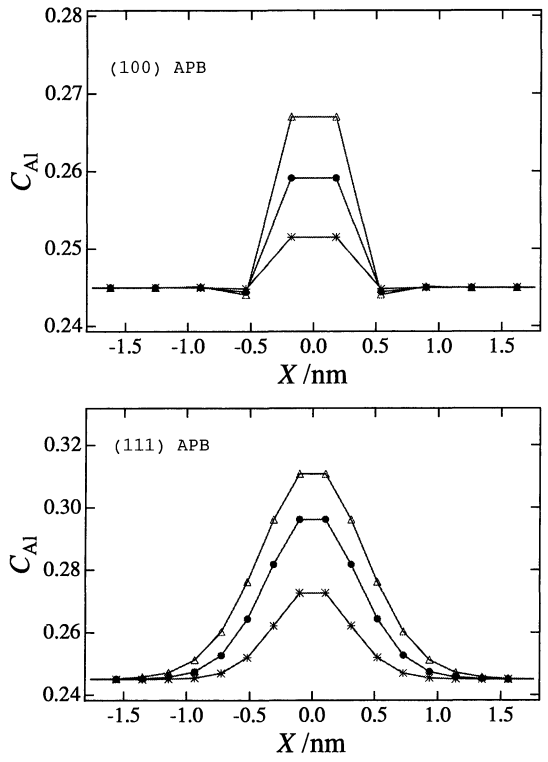

Fig. 2 Al concentration C_{Al} as a function of the distance X to the center of the APB in $Ni_{0.725}Al_{0.245}Ti_{0.010}$ (*), $Ni_{0.735}Al_{0.245}Ti_{0.020}$ (●), and $Ni_{0.725}Al_{0.245}Ti_{0.030}$ (△), at a temperature of 2000 K. Upper figure is for (100) APB, and lower for (111).

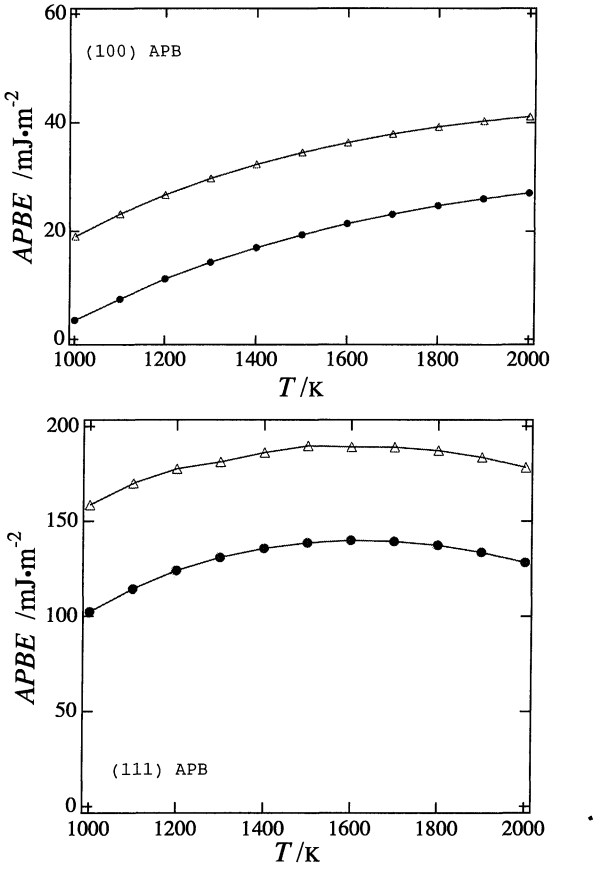

Fig. 3 APBE as a function of temperature in $Ni_{0.745}Al_{0.245}Ti_{0.010}$ (△) and in $Ni_{0.725}Al_{0.255}Ti_{0.020}$ (●). Upper figure is for (100) APB, and lower for (111).

APB to increase its APBE.

The APBE appears to have a maximum as a function of temperature. That means that the excess entropy associated with the APB is negative at low temperature, and becomes positive at high temperature. At low temperature the APB excess entropy is negative because the APB acts as a sink for defects. Off-stoichiometry and anti-site defects segregate towards the APB and thereby reduce the configurational entropy, because these defects are now distributed in a much smaller area. At high temperature, defects do not segregate so strongly, and another effect dominates. Around the APB there is then a wide region where the order parameter is much smaller than in the rest of the crystal. Such a region contributes a large configurational entropy, so that the total excess entropy due to the APB takes a positive value.

The slight difference in the temperature dependence of (100) and (111) APBs can now be understood. The segregation towards (111) APBs is stronger than towards (100) APBs, so that the (111) APB entropy is larger at low temperature. However, at high temperature the region with reduced order too, is much wider around (111) APBs. But more importantly, the disordering starts at a lower temperature at (111) APBs than at (100) APBs because the energy associated with the (111) APB is so much larger. Therefore, the (111) APBE reaches its maximum value at a lower temperature than the (100) APBE, which is readily apparent in Fig. 3.

The (111) APBE in Ni_3Al has been determined experimentally with the weak beam method[22]. This measurement indicates that APBEs increase when early transition metals[22], such as Ti, V, and Hf, are added to Ni_3Al. Although the experimental results are fragmentary, it appears that the effect could be significant. A (111) APBE of 150 mJ/m^2 in $Ni_{0.757}Al_{0.227}Hf_{0.016}$ was measured and 190 mJ/m^2 in $Ni_{0.7704}Al_{0.2270}Hf_{0.0026}$, and a similar difference occurred for the (100) APBE. This has been interpreted to mean that Hf strongly increases the APBE. As is well-known from the Gibbs absorption equation[23][24] these findings indicate that early transition metal impurities in Ni_3Al segregate away from the APBs. Our findings for Ti are in complete agreement with these observations.

IV. Conclusion

Order-disorder and segregation effects were computed with the CVM in the TO approximation for $Ni_{3-x}Al_{1-y}Ti_{x+y}$ alloys. Effective interatomic interactions derived from *ab initio* LDA electronic structure calculations were used. It was found that the APBE in $L1_2$ compounds is generally larger on (111) planes than on (100) planes, and an explanation in terms of the ECI was given. It was shown that Ti strongly segregates away from APBs and this was explained in terms of the strong

site preference which is driven by the ECI. Our work suggests that quite generally substitutional impurities that have a strong Al-site preference are likely to segregate away from the APB. Similarly, it was shown that in comparison to (100) APBs, segregation is strong and the segregated zone is wide for (111) APBs. This could be explained based on the stronger coupling between (111) planes. The same reasoning was applied to the finding that the maximum of the APBE with temperature was reached at a lower temperature for (111) APBs. It was shown that the segregation of Ti away from the APB, caused Al to more strongly segregate towards the APB. As such, Ti can be said to increase segregation tendencies at APBs in Ni–Al–Ti alloys. It was shown that addition of Ti increases the APBE. Possibly, other early transition metals which have a similar strong Al site preference behave much like Ti.

Acknowledgements

The authors gratefully acknowledge the help from the staff at the Computer Center at IMR, Tohoku University with the use of the Hitachi S-3800 supercomputer. One of us (HPW) wishes to acknowledge the kind help given by all of the members in Kawazoe's Laboratory of the Institute for Materials Research, Tohoku University.

REFERENCES

(1) D. L. Anton: *Intermetallic Compounds Principles and Practice*, Volume 2, *Practice*, ed. by J. H. Westbrook and R. L. Fleischer, Wiley, NY, (1995), pp. 3-15.
(2) J. L. C. Daams, P. Villars and J. H. N. van Vucht: *Atlas of crystal structures for intermetallic phases*, ASM International, Materials Park OH, (1991), pp. 6402-6404.
(3) D. M. Dimiduk, A. W. Thompson and J. C. Williams: Phil. Mag. **A, 67** (1993), 675-698.
(4) M. Sluiter and Y. Kawazoe: Phil. Mag. **A, 78**, No. 6 (1998), 1353-1364.
(5) M. Sluiter and Y. Kawazoe: Phys. Rev. **B, 51** (1995), 4062-4073.
(6) M. Sluiter, M. Takahashi and Y. Kawazoe: Acta Metall., **44** (1996), 209-215.
(7) D. de Fontaine: in *Solid State Physics*, Vol. **34**, ed. by H. Ehrenreich, F. Seitz and D. Turnbull, Academic Press, New York, (1979), 73-274.; D. de Fontaine: in *Solid State Physics*, Vol. **47**, ed. by H. Ehrenreich and D. Turnbull, Academic Press, New York, (1994), pp. 80-176.
(8) M. Sluiter, Y. Watanabe, D. de Fontaine and Y. Kawazoe: Phys. Rev. B, **53** (1996), 6137-6151.
(9) H. L. Skriver: *The LMTO Method*, Springer Series in Solid State Sciences, Vol. **41**, Springer, Heidelberg, (1983), pp. 1-260; O. K. Anderson, O. Jepsen, and D. Glotzel, in *Highlights of Condensed Matter Theory*, Internat. School of Phys. Enrico Fermi, Course **89**, eds. by F. Bassani, F. Fermi and M. P. Tosi, North Holland, Amsterdam, (1985), pp. 59-176. (The actual code was graciously provided by Dr. M. van Schilfgaarde).
(10) H. J. Monkhorst and J. D. Pack: Phys. Rev. B, **13** (1976), 5188-5192.
(11) M. Sluiter, M. Takahashi and Y. Kawazoe: J. Alloys and Compounds, **248** (1997), 90-97.
(12) M. Sluiter, K. Esfarjani and Y. Kawazoe: Phys. Rev. Lett., **75** (1995), 3142-3145.
(13) J.-Z. Yu, M. Sluiter and Y. Kawazoe: Sci. Rep. RITU, Ser., **A41** (1996), 153-155.
(14) R. W. Cahn: in *High Temperature Ordered Intermetallic Alloys II*, ed. N.S. Stoloff *et al.*, Mater. Res. Soc. Proc., **81** (1987), pp. 27-38.
(15) D. M. Dimiduk, S. Rao, T. A. Parthasarathy and C. Woodward: in *Ordered Intermetallics-Physical Metallurgy and Mechanical Behavior*, ed. C. T. Liu *et al.*, Kluwer, Dordrecht, Netherlands, (1992), pp. 237-248.
(16) S. P. Chen, A. F. Voter and D. J. Srolovitz: Scripta Metall., **20** (1986), pp. 1389-1394.
(17) S. M. Foiles and M. S. Daw: J. Mater. Res., **2** (1987), 5-15.
(18) C. L. Fu and M. H. Yoo: in *High Temperature Ordered Intermetallic Alloys III*, ed. C. T. Liu *et al.*, Mater. Res. Soc. Proc., **133** (1989), pp. 81-86.
(19) C. L. Fu, Y.-Y. Ye and M. H. Yoo: in *High Temperature Ordered Intermetallic Alloys V*, ed. I. Baker *et al.*, Mater. Res. Soc. Proc., **288** (1993), pp. 21-28.
(20) A. T. Paxton: in *Electron Theory and Alloys Design*, ed. by D. Pettifor and A. Cottrell, Alden Press, Oxford, UK, (1992), pp. 158-190.
(21) C. L. Fu: Phys. Rev. **B, 52** (1995), 3151-3158.
(22) Y.-Q. Sun: in *Intermetallic Compounds: Principles and Practice*, eds. by J. H. Westbrook and R. L. Fleischer, vol. **1**, (1995), pp. 495-517, (Wiley & Sons, NY); and references therein.
(23) W. J. Moore: *Physical Chemistry*, Longman, London, (1976), pp. 484-487.
(24) A. P. Sutton and R. W. Baluffi: *Interfaces in Crystalline Materials*, Monographs on the Physics and Chemistry of Materials, Clarendon Press, Oxford, U.K., (1995), pp. 414-423.